Mon. Not. R. Astron. Soc. **000**, 000–000 (0000) Printed 27 August 2014 (MN LATEX style file v2.2)

# Helium enrichment and Carbon-star Production in Metal-rich Populations

Amanda I. Karakas[1,2⋆]
[1] *Research School of Astronomy and Astrophysics, Australian National University, Canberra, ACT 2611, Australia*
[2] *Kavli Institute for the Physics and Mathematics of the Universe (WPI), Todai Institutes for Advanced Study, The University of Tokyo, Japan*

arXiv:1408.5936v1 [astro-ph.SR] 25 Aug 2014

**ABSTRACT**
We present new theoretical stellar evolutionary models of metal-rich asymptotic giant branch (AGB) stars. Stellar models are evolved with initial masses between $1M_{\odot}$ and $7M_{\odot}$ at $Z = 0.007$, and $1M_{\odot}$ and $8M_{\odot}$ at $Z = 0.014$ (solar) and at $Z = 0.03$. We evolve models with a canonical helium abundance and with helium enriched compositions ($Y = 0.30, 0.35, 0.40$) at $Z = 0.014$ and $Z = 0.03$. The efficiency of third dredge-up and the mass range of carbon stars decreases with an increase in metallicity. We predict carbon stars form from initial masses between 1.75–$7M_{\odot}$ at $Z = 0.007$ and between 2–$4.5M_{\odot}$ at solar metallicity. At $Z = 0.03$ the mass range for C-star production is narrowed to 3.25–$4M_{\odot}$. The third dredge-up is reduced when the helium content of the model increases owing to the reduced number of thermal pulses on the AGB. A small increase of $\Delta Y = 0.05$ is enough to prevent the formation of C stars at $Z = 0.03$, depending on the mass-loss rate, whereas at $Z = 0.014$, an increase of $\Delta Y \gtrsim 0.1$ is required to prevent the formation of C stars. We speculate that the probability of finding C stars in a stellar population depends as much on the helium abundance as on the metallicity. To explain the paucity of C stars in the inner region of M31 we conclude that the observed stars have $Y \gtrsim 0.35$ or that the stellar metallicity is higher than [Fe/H] $\approx 0.1$.

**Key words:** stars: abundances, evolution, AGB and post-AGB, carbon, Galaxy: abundances, bulge, galaxies: abundances, M31

## 1 INTRODUCTION

The bulge of the Milky Way Galaxy is home to some of the oldest and most metal-rich stars in our Galaxy. While most of the stars in the bulge are consistent with being older than 10 Gyr (e.g., Ortolani et al. 1995; Zoccali et al. 2003; Brown et al. 2010; Valenti et al. 2013), there is evidence for a spread in ages with the youngest stars having ages as low as 2 Gyr (Bensby et al. 2013). The bulge is also home to a number of planetary nebulae (PNe) and asymptotic giant branch (AGB) stars (van Loon et al. 2003; Cole & Weinberg 2002; Górny et al. 2004; Groenewegen & Blommaert 2005; Uttenthaler et al. 2007; Górny et al. 2010; García-Hernández & Górny 2014). The AGB stars show evidence of self enrichment through dredge-up processes owing to the detection of the heavy element technetium (Tc), although they themselves are not carbon rich (Uttenthaler et al. 2007, 2008). Tc is a product of the slow neutron capture process, the *s*-process, which occurs in the deep interiors of AGB stars and is mixed to the surface by the third dredge-up. The third dredge-up takes place after a thermal pulse and can occur many times, depending on the initial mass, metallicity, and H-exhausted core mass (for reviews of AGB evolution and nucleosynthesis we refer to Busso et al. 1999; Herwig 2005; Karakas & Lattanzio 2014). However the dominant product of the third dredge-up is carbon, which is produced as a primary product of helium burning by the triple-alpha process. The third dredge-up therefore mixes carbon and heavy elements to the surface, and is the mechanism for converting oxygen-rich AGB stars to carbon-rich stars, which have more carbon than oxygen atoms in their atmospheres, that is, C/O $\geqslant 1$ (e.g., Wallerstein & Knapp 1998).

The fact that the bulge AGB stars are rich in Tc means that the third dredge-up has occurred, which requires a minimum mass of about $\gtrsim 1.5M_{\odot}$. Cole & Weinberg (2002) found a population of carbon stars that traced the bar of our Galaxy and speculated that some of these may have wandered into the bulge region. The bulge PNe on the other hand show a double chemistry, with oxygen bearing molecules found together with polycyclic aromatic hydrocarbons, which are carbon-bearing molecules. While the double chemistry phenomena may be the re-

⋆ E-mail: amanda.karakas@anu.edu.au

sult of chemical reactions and not internal nucleosynthesis (Guzman-Ramirez et al. 2011), spectroscopic follow-up observations of bulge PNe find that some of them have experienced the third dredge-up (García-Hernández & Górny 2014). The progenitor masses of the PNe are not known, with García-Hernández & Górny (2014) speculating that some of the nebula evolved from intermediate-mass AGB stars with masses $\geqslant 4M_{\odot}$.

While the metallicity distribution of stars in the Galactic bulge shows a tail down to [Fe/H] $\lesssim -2$[1], the mean metallicity is around solar (e.g., Zoccali et al. 2008; Bensby et al. 2013), with 95% of stars near the plane having metallicities between $-1 \lesssim$ [Fe/H] $\lesssim 0.6$ (Bensby et al. 2013). The bulge has been shown to comprise two or three metallicity components, peaked at above solar ([Fe/H] $\approx 0.1 - 0.3$) and just below solar metallicity with the metal-rich stars closer to the plane (Babusiaux et al. 2010; Hill et al. 2011; Ness et al. 2013). Bensby et al. (2013) find the younger stellar component resides in the metal-rich bulge. The $\alpha$-element content of the metal-rich bulge is approximately solar or within 0.2 dex of solar for Mg, Si, Ca, and Ti (Hill et al. 2011; Bensby et al. 2013) although [O/Fe] declines linearly with [Fe/H] (see also Johnson et al. 2011; Gonzalez et al. 2011). If the AGB stars and PNe are truly in the bulge, they likely evolved from a relatively young and metal-rich stellar population with [Fe/H] $\geqslant 0.0$ and [$\alpha$/Fe] $\approx 0$.

Dredge-up in AGB stars is strongly dependent on metallicity as well as mass (e.g., Boothroyd & Sackmann 1988; Karakas et al. 2002; Straniero et al. 2003), with lower dredge-up efficiencies found at solar metallicity compared to the metallicities of the Magellanic Clouds. However, the studies by Karakas, Lattanzio, & Pols (2002) and Straniero et al. (2003) did not include AGB stars with metallicities higher than solar so it is unclear how dredge-up efficiencies vary as a function of mass in super-solar metallicity AGB stars. The high initial oxygen abundance of metal-rich stars further impedes the formation of carbon stars, because carbon star formation requires there to be enough carbon atoms to exceed the now high number of oxygen atoms. These two factors have led to the suggestion that there is a metallicity ceiling to carbon-star formation, as discussed by Boyer et al. (2013) in the context of a paucity of carbon stars in the inner region of the Andromeda Galaxy (M31).

Helium enrichment may also be an important factor for stars in the bulges of spiral galaxies and in early-type galaxies (Atlee et al. 2009; Nataf et al. 2011; Chung et al. 2011; Nataf & Gould 2012; Rosenfield et al. 2012; Buell 2013) In order to reconcile the factor $\approx 2$ discrepancy between spectroscopic and photometric age determinations of the Galactic bulge main-sequence turnoff, Nataf & Gould (2012) suggested that the metal-rich component of the bulge may also be helium rich, with helium abundances $\Delta Y \approx 0.1$ up from canonical expectations[2]. Bensby et al. (2013) note that an increase of helium by 0.1 does not remove the need for a young and intermediate-age stellar population. HST photometry has also revealed that some Galactic Globular Clusters also host helium-rich populations, with helium abundances up to $Y \approx 0.4$ in the case of $\omega$ Centauri and NGC 2808 (e.g., Norris 2004; Piotto et al. 2005; D'Antona et al. 2005; Joo & Lee 2013).

The effect of helium-enrichment on stellar evolution during the giant branches is less well understood than its effect on colour-magnitude diagrams. Karakas, Marino, & Nataf (2014) studied the effect of helium enrichment on the evolution and nucleosynthesis of low-mass AGB stars. Helium enrichment was found to severely reduce the stellar yields expected from low-mass AGB populations at low metallicities by more than 50% for some elements. The effect at solar or super-solar metallicities is not known. Note that the origin of the high helium abundances is unknown, although it has been speculated that low-metallicity intermediate-mass or super-AGB stars or massive stars produced the high helium content of Galactic Globular Clusters (e.g., Norris 2004; Karakas et al. 2006; D'Ercole et al. 2012).

The aim of the present study is to provide new detailed stellar evolutionary models of low and intermediate-mass AGB stars of updated solar metallicity ($Z = 0.014$) and super-solar metallicity ($Z = 0.03$). These models will be used to provide the first study of the dependence on mass and helium abundance on the third dredge-up at $Z = 0.03$, and will be useful for a range of applications including synthetic or parametric AGB studies (e.g., Izzard et al. 2004; Marigo et al. 2013; Buell 2013). We also map out the mass range of carbon stars at super-solar metallicities from detailed stellar evolution models, and examine the effect of helium enrichment on the predicted mass range of carbon stars. Given that a large initial helium abundance truncates the yields of low mass, lower metallicity AGB models (Karakas et al. 2014), it is reasonable to expect that enhanced helium may inhibit carbon star production at higher metallicities. In this paper we first introduce the stellar evolutionary models in §2 including a discussion of the initial helium abundance. We then present the results of the new stellar models in §3 including a comparison to other studies, discuss the major uncertainties affecting the results in §4, and finish with a discussion and conclusions in §5.

## 2 STELLAR EVOLUTIONARY MODELS

In this study we evolve stellar models of mass $1M_{\odot}$ to $7M_{\odot}$ with a global metallicity of $Z = 0.007$, and $1M_{\odot}$ to $8M_{\odot}$ with metallicities of $Z = 0.014$ (solar) and $Z = 0.03$. The full grid of masses at each metallicity is given in Table 1. Models are evolved from the pre-main sequence to the tip of the AGB. The maximum masses at each metallicity experience off-centre carbon ignition but the carbon burning does not reach the centre. These are CO(Ne) core AGB stars according to the definitions given in Karakas & Lattanzio (2014) and are not true super-AGB stars, which have O-Ne cores (e.g., Siess 2010; Doherty et al. 2010). The metallicities were chosen so we include models of solar metallicity and a metallicity that is approximately a factor of two more metal-poor and metal-rich than solar.

The metallicities of the models are representative of disc metallicities, according to iron abundances derived

[1] where we use the standard spectroscopic notation [Fe/H] = $\log_{10}(\mathrm{Fe/H})_{*} - \log_{10}(\mathrm{Fe/H})_{\odot}$.

[2] where $Y$ is the mass fraction of helium, $X$ the mass fraction of hydrogen and $Z$ the mass fraction of metals. $Z$ is also the global metallicity of the stellar model.

from stars (Edvardsson et al. 1993; Casagrande et al. 2011; Bensby et al. 2014; Recio-Blanco et al. 2014), and abundances of oxygen and zinc in planetary nebulae, which are tracers of Galactic disc metallicities (e.g., Stasińska et al. 1998; Stanghellini & Haywood 2010; Smith et al. 2014). The solar and metal-rich models are appropriate for comparison to stars and planetary nebulae in the metal-rich bulge of our Milky Way Galaxy (Bensby et al. 2013; Ness et al. 2013), and also for comparison to AGB stars found in the inner regions of spiral galaxies such as M31 (Saglia et al. 2010; Boyer et al. 2013). The lower metallicity models of $Z = 0.007$ (or [Fe/H] $\approx -0.3$) are similar to the the metallicity of thick disc (e.g., Reddy et al. 2006; Recio-Blanco et al. 2014) or the peak metallicity of the Large Magellanic Cloud (LMC, Cole et al. 2005), and will mostly be used here for comparison to the metal-rich models.

The input physics used in the stellar evolutionary sequences is exactly the same as described in Karakas et al. (2014). The initial composition of C, N, and O are scaled solar in the $Z = 0.03$ and $Z = 0.007$ models and solar in the $Z = 0.014$ models, where the solar abundances are from Asplund et al. (2009). We choose to use the Asplund et al. (2009) abundances for comparison to other recent solar-metallicity stellar evolution models (e.g., by Cristallo et al. 2011; Ekström et al. 2012, who adopt $Z = 0.014$ or a value close to that). Furthermore, we show in §4 that the stellar evolution calculations are not dependent on the choice of solar abundances and that adopting the say, Lodders et al. (2009) solar abundances, which have $Z_\odot = 0.0153$, does not change the results for a $3M_\odot$ model. In the $Z = 0.007$ models we assume a scaled-solar composition, noting that there is little or no $\alpha$-enhancement in the Galactic thin disc at [Fe/H] $= -0.3$ and only a mild $\alpha$-enhancement in the thick disc at these metallicities (e.g., Figs. 12 and 13 from Reddy et al. 2006).

The initial helium abundance is varied in the solar and metal-rich models ($Z = 0.014, 0.03$, respectively) and is described in more detail below. We assume no mass loss on the red giant branch (RGB) and use the Vassiliadis & Wood (1993) mass-loss formulation on the AGB. While the assumption of no mass loss on the RGB is an incorrect assumption, the Kepler results by Miglio et al. (2012) suggest that the mass-loss rates in metal-rich open cluster giant stars are less than predicted by Reimer's type mass-loss prescriptions with $\eta \approx 0.4$. We use the C and N-rich low-temperature opacity tables from Marigo & Aringer (2009), which are based on the solar composition of Lodders (2003). The OPAL tables use the same initial composition as the low-temperature tables for consistency. We note that the initial solar $Z$ is slightly lower in the opacity tables than we assume here in the stellar evolutionary calculations ($Z = 0.01321$ in the opacity tables compared to 0.014) but the difference is small ($\Delta Z = 0.00079$).

Convection is approximated using the Mixing-length Theory with a mixing-length parameter of $\alpha = 1.86$ in all calculations. No convective overshoot is applied although we use the algorithm described by Lattanzio (1986) to search for a neutrally stable point for the border between convective and radiative zones. This has been shown to increase the amount of third dredge-up relative to models that set the position of the convective border according to the formal Schwarzschild boundary (Frost & Lattanzio 1996; Mowlavi 1999). Kamath, Karakas, & Wood (2012) found that this scheme was not able to reproduce the observations of AGB stars in Magellanic Cloud clusters and further mixing was required. Kamath et al. (2012) required a large amount of convective overshoot (up to 3 pressure scale heights) at the base of the convective envelope during third dredge-up in order to match the O-rich to C-rich transition luminosity of the cluster AGB stars. Here we ignore further mixing until §3.3, noting this is a considerable uncertainty to the lower mass limit for carbon star production.

### 2.1 The initial helium abundance

The primordial helium abundance, $Y_\mathrm{p}$, is a firm lower limit to the initial abundance of helium of the first stars in the Universe. For other generations of stars, the helium abundance has been steadily increasing as a result of stellar nucleosynthesis and is determined according to:

$$Y = \frac{\Delta Y}{\Delta Z} Z + Y_\mathrm{p}, \quad (1)$$

where $\Delta Y/\Delta Z$ is the rate of helium production and is typically expressed relative to the change in metallicity, $Z$. Both $Y_\mathrm{p}$ and the gradient can be estimated from observations. Aver et al. (2013) estimate a value for $Y_\mathrm{p} = 0.2485 \pm 0.0002$, based on the Planck determination of the baryon density and using the most recent He I emissivities based on improved photoionization cross-sections from Porter et al. (2012), and a re-analysis of the observations by Izotov et al. (2007). The slope, $\Delta Y/\Delta Z$, has been estimated to be between 1 to 10 (Chiappini et al. 2002; Balser 2006; Gennaro et al. 2010; Portinari et al. 2010), with Balser (2006) finding a value of $1.41 \pm 0.62$ in the Galaxy, consistent with standard chemical evolution models (e.g., Chiappini et al. 2002). Izotov et al. (2007) estimate a value closer to 3 (2.94 or 2.88, depending upon their choice of He I emissivities) for low metallicity extra-galactic HII regions, whereas Casagrande et al. (2007) estimate $\Delta Y/\Delta Z$ to be $2.1 \pm 0.9$ around and above solar metallicity.

In the models with global metallicities set to $Z = 0.014$ and $Z = 0.03$, we investigate the effect of varying the initial helium abundance on the stellar evolutionary sequences, and in particular, on the evolution during the AGB. In the $Z = 0.014$ models we set our canonical value $Y = 0.28$ and in the $Z = 0.03$ models we set the canonical $Y = 0.30$ (where $X + Y + Z = 1$, noting that when we vary $Y$ we keep $Z$ constant, which means that the hydrogen abundance, $X$, also varies). We set $Y = 0.26$ in all the $Z = 0.007$ models. We then evolve a series of models with masses between $2M_\odot$ and $5M_\odot$ at $Z = 0.014$ and $Z = 0.03$ with helium abundances shown in Table 2. The mass range of models was chosen to investigate the effect of helium enrichment on the production of carbon stars.

If we take $Y_\mathrm{p} = 0.2485$ (Aver et al. 2013) and $\Delta Y/\Delta Z = 2.1$ (Casagrande et al. 2007), then at $Z = 0.007, 0.014$ and $Z = 0.03$ we get $Y = 0.2632, 0.2779$, and $Y = 0.3115$, respectively. These are close to our chosen canonical values at our metallicities although it suggests that our choice of $Y = 0.28$ is a bit high for solar metallicity, which is motivation to run a few models with a lower value of $Y = 0.26$. For the $Z = 0.03$ models, the standard helium abundance of $Y = 0.30$ is a bit low for metal-rich

stars, which is motivation for calculating a few stellar models with initial helium of $Y = 0.32$. Helium-enriched models at both metallicities include those calculated with $Y = 0.35$ and $Y = 0.40$. Note that at $Z = 0.014$, an initial helium of $Y = 0.35$ or 0.40 implies a slope of $\Delta Y/\Delta Z = 7.25$ and 10.82, respectively, whereas at $Z = 0.03$ the slope is 3.38 and 5.05 for $Y = 0.35$ and 0.40.

## 3 RESULTS

In Tables 1 and 2 we present the list of stellar models calculated for this study. We note if the second (SDU) or third dredge-up (TDU) occur and if hot bottom burning (HBB) is active. We include the total number of thermal pulses (#TP), the final C/O ratio in the envelope (by number), the maximum third dredge-up efficiency, $\lambda_{\rm max}$, the H-exhausted core mass (hereafter core mass) at the first thermal pulse, $M_{\rm c}(1)$, the core mass at the first third dredge-up episode, $M_{\rm c}^{\rm min}$, the maximum temperature at the base of the convective envelope, $T_{\rm bce}^{\rm max}$, the maximum luminosity on the TP-AGB, $L_{\rm agb}^{\rm max}$, the total stellar lifetime, $\tau_{\rm stellar}$, the lifetime on the AGB including early-AGB, $\tau_{\rm agb}$, the lifetime on the TP-AGB, $\tau_{\rm tpagb}$, the lifetime during the C-rich phase, $\tau_{\rm c}$, and the ratio between the C-rich lifetime and the lifetime on the AGB, $(\tau_{\rm c})/(\tau_{\rm agb})$.

The third dredge-up efficiency is defined according to $\lambda = \Delta M_{\rm dredge}/\Delta M_{\rm core}$, where $\lambda$ is the third dredge-up efficiency parameter, $\Delta M_{\rm dredge}$ is the mass mixed into the envelope, and $\Delta M_{\rm core}$ is the amount by which the H-exhausted core increases over the previous interpulse phase. Masses and luminosities are in solar units, temperatures in $10^6$ K, and ages in Myr.

We define low-mass stars as those that experience the core helium flash and intermediate-mass stars as those that ignite helium under non-degenerate conditions. The maximum mass for the core helium flash is $2{\rm M}_\odot$ at $Z = 0.007$, $2.25{\rm M}_\odot$ at $Z = 0.014$ and $2.5{\rm M}_\odot$ at $Z = 0.03$. Note that we do not include a model of $2{\rm M}_\odot$ at $Z = 0.007$ owing to convergence difficulties during core He ignition. All models experience the FDU. The SDU requires a minimum H-exhausted core mass of $0.8{\rm M}_\odot$ on the early AGB and this is satisfied by models of $4.5{\rm M}_\odot$ at $Z = 0.014$ and $5{\rm M}_\odot$ at $Z = 0.03$. At $Z = 0.007$ the SDU starts at $4{\rm M}_\odot$, although it is very shallow at this mass. The effect of the first and second dredge-up is to lower the C/O ratio from its initial value (which we assume is solar, C/O = 0.55) to C/O $\lesssim 0.3$, as well as decreasing the $^{12}{\rm C}/^{13}{\rm C}$ ratio.

HBB occurs during the TP-AGB when the base of the convective envelope becomes hot enough for CNO cycle reactions to occur, and can produce significant increases to the luminosity and changes to the surface abundances (for more details we refer to reviews by Herwig 2005; Karakas & Lattanzio 2014). Of importance for this study is the effect HBB can have on preventing the formation of a carbon-rich atmosphere, by converting $^{12}$C to $^{14}$N (Boothroyd et al. 1993). Once HBB ceases, dredge-up can continue and the star may still become C-rich (Frost et al. 1998; van Loon et al. 1999). This is observed in our lowest metallicity models, where all intermediate-mass models become C-rich. HBB begins to alter the surface composition when the temperature exceeds $50 \times 10^6$ K (MK), which is reached in models of $4.25{\rm M}_\odot$ at $Z = 0.007$, $4.5{\rm M}_\odot$ at $Z = 0.014$, and $5{\rm M}_\odot$ at $Z = 0.03$ (Table 1).

Karakas et al. (2014) discussed the effect of helium enrichment on the stellar lifetimes and core masses in low-mass, low metallicity AGB models. They found that an increase in the initial helium abundance leads to a shorter stellar lifetime, as a consequence of less hydrogen fuel for the main sequence. Stellar lifetimes are reduced in the helium-rich and metal-rich models, where the total lifetimes decreases by factors of $1.7 - 2.0$, depending on initial mass and helium abundance (see Tables 1 and 2). The total stellar lifetime of a $3{\rm M}_\odot$, $Z = 0.03$ model is reduced from 530 Myr when $Y = 0.30$ to 283 Myr when $Y = 0.40$, a decrease of 47% and we see similar reductions in the solar metallicity model of the same mass. AGB lifetimes are reduced by factors of 2.0-3.0, again depending upon mass and helium composition. The implication here is that AGB stars located in the (helium-rich) bulges of galaxies may not be as old as estimated from canonical stellar evolutionary calculations.

An increase in the core mass on the beginning of the AGB means that the minimum core mass for the occurrence of the SDU and HBB is lowered in helium-rich models (Karakas et al. 2014). The minimum mass for the SDU is reduced from $4{\rm M}_\odot$ to $3.5{\rm M}_\odot$ at $Z = 0.014$ when $Y = 0.35$. Similarly, the minimum mass for HBB is reduced from $4.5{\rm M}_\odot$ to $4{\rm M}_\odot$ at $Z = 0.014$. At $Z = 0.03$, the minimum mass for SDU drops from $4.5{\rm M}_\odot$ to $4{\rm M}_\odot$ although the minimum mass for HBB does not change. The effect of HBB on the evolution of the surface C/O ratio is weak at the minimum mass; the reduction in third dredge-up efficiency and the decrease in the AGB lifetimes are more important, as we discuss next.

### 3.1 The third dredge-up

In Figure 1 we show a comparison between the new $Z = 0.014$ and $Z = 0.03$ models with a canonical helium abundance to the parametrization of the third dredge-up for $Z = 0.02$ provided by Karakas et al. (2002). We also include the model data for the $Z = 0.02$ models with mass loss from that study. The $Z = 0.02$ fit is an excellent match to the core mass at the first thermal pulse for the $Z = 0.014$ models and for the $Z = 0.03$ models for $M \leqslant 3{\rm M}_\odot$. The core mass at the first thermal pulse is smaller in the $Z = 0.03$ for $3.25 \leqslant M({\rm M}_\odot) \leqslant 6$ compared to the fit. This mass range experiences the deepest third dredge-up, as shown by by Figure 1 (c). Similar to the results found by Karakas et al. (2002), we find that the core mass at the first thermal pulse is a good approximation for the core mass at the first TDU episode for $M > 4{\rm M}_\odot$. The core mass at the first thermal pulse and at the first TDU episode are larger in the $8{\rm M}_\odot$ models than the parameterization by Karakas et al. (2002). This is not entirely surprising as the fit was made using models with a maximum mass of $6{\rm M}_\odot$ (although it does do a good job for the $7{\rm M}_\odot$ models).

Karakas et al. (2002) used solar metallicity models without mass loss to derive the fits shown in Figure 1. Our new $Z = 0.014$ models are a good match to those fits. In comparison, the $Z = 0.02$ models with mass loss from Karakas et al. (2002) have shallower dredge-up for $M \leqslant 2.5{\rm M}_\odot$. The $Z = 0.03$ models show similar values to $\lambda_{\rm max}$ as the $Z = 0.014$ models for $M \geqslant 3.5{\rm M}_\odot$; however the

**Table 1.** Stellar models calculated with a canonical helium composition. The luminosity is in the format $n(m)$ where $= n \times 10^m L_\odot$.

| Mass ($M_\odot$) | SDU | HBB | TDU | #TP | $C/O_f$ | $\lambda_{max}$ | $M_c(1)$ ($M_\odot$) | $M_c^{min}$ ($M_\odot$) | $T_{bce}^{max}$ (MK) | $L_{agb}^{max}$ ($L_\odot$) | $\tau_{stellar}$ (Myr) | $\tau_{agb}$ (Myr) | $\tau_{tpagb}$ (Myr) | $\tau_c$ (Myr) | $\tau_c/\tau_{agb}$ |
|---|---|---|---|---|---|---|---|---|---|---|---|---|---|---|---|
| $Z = 0.007$, $Y = 0.26$ models. | | | | | | | | | | | | | | | |
| 1.00 | No | No | No | 15 | 0.463 | 0.00 | 0.537 | – | 1.75 | 5.69(3) | 10065 | 20.66 | 1.875 | – | – |
| 1.25 | No | No | No | 16 | 0.403 | 0.00 | 0.545 | – | 2.28 | 6.99(3) | 4526 | 19.23 | 1.921 | – | – |
| 1.50 | No | No | Yes | 19 | 0.509 | 0.10 | 0.549 | 0.636 | 2.78 | 8.55(3) | 2451 | 18.70 | 2.112 | – | – |
| 1.75 | No | No | Yes | 20 | 1.566 | 0.49 | 0.554 | 0.638 | 3.19 | 9.98(3) | 1535 | 17.28 | 2.155 | 0.137 | 0.008 |
| 1.90 | No | No | Yes | 21 | 2.475 | 0.52 | 0.552 | 0.615 | 3.45 | 9.64(3) | 1216 | 17.69 | 2.193 | 0.317 | 0.018 |
| 2.10 | No | No | Yes | 24 | 3.397 | 0.60 | 0.538 | 0.617 | 3.63 | 9.44(3) | 968.5 | 21.13 | 2.801 | 0.494 | 0.023 |
| 2.25 | No | No | Yes | 27 | 4.254 | 0.68 | 0.532 | 0.608 | 3.92 | 1.06(4) | 900.2 | 23.72 | 3.185 | 0.662 | 0.028 |
| 2.50 | No | No | Yes | 27 | 5.389 | 0.76 | 0.555 | 0.609 | 4.64 | 1.14(4) | 687.3 | 17.06 | 2.621 | 0.897 | 0.053 |
| 3.00 | No | No | Yes | 22 | 6.820 | 0.87 | 0.649 | 0.658 | 7.25 | 1.36(4) | 394.8 | 8.239 | 1.361 | 0.935 | 0.114 |
| 3.50 | No | No | Yes | 21 | 5.812 | 0.97 | 0.746 | 0.750 | 17.8 | 1.72(4) | 256.8 | 4.770 | 0.670 | 0.503 | 0.105 |
| 4.00 | Yes | No | Yes | 24 | 4.144 | 0.98 | 0.837 | 0.839 | 46.1 | 2.28(4) | 181.7 | 2.984 | 0.350 | 0.251 | 0.084 |
| 4.25 | Yes | Yes | Yes | 28 | 3.563 | 0.97 | 0.846 | 0.849 | 56.5 | 2.47(4) | 155.1 | 2.625 | 0.358 | 0.248 | 0.095 |
| 4.50 | Yes | Yes | Yes | 50 | 1.118 | 0.96 | 0.856 | 0.858 | 76.4 | 3.19(4) | 134.9 | 2.352 | 0.543 | 0.014 | 0.006 |
| 5.00 | Yes | Yes | Yes | 59 | 1.881 | 0.95 | 0.876 | 0.878 | 82.9 | 3.69(4) | 104.3 | 1.736 | 0.500 | 0.023 | 0.013 |
| 5.50 | Yes | Yes | Yes | 67 | 1.947 | 0.93 | 0.902 | 0.903 | 86.8 | 4.17(4) | 83.54 | 1.270 | 0.408 | 0.018 | 0.014 |
| 6.00 | Yes | Yes | Yes | 64 | 2.075 | 0.92 | 0.940 | 0.941 | 92.0 | 4.75(4) | 68.89 | 0.846 | 0.259 | 0.017 | 0.021 |
| 7.00 | Yes | Yes | Yes | 61 | 2.040 | 0.90 | 1.030 | 1.031 | 102 | 6.15(4) | 48.93 | 0.117 | 0.096 | 0.004 | 0.038 |
| $Z = 0.014$, $Y = 0.28$ models. | | | | | | | | | | | | | | | |
| 1.00 | No | No | No | 12 | 0.469 | 0.00 | 0.546 | – | 1.77 | 4.81(3) | 12186 | 21.34 | 1.100 | – | – |
| 1.25 | No | No | No | 14 | 0.412 | 0.00 | 0.550 | – | 2.39 | 6.00(3) | 5372 | 19.55 | 1.286 | – | – |
| 1.50 | No | No | No | 17 | 0.380 | 0.00 | 0.555 | – | 2.76 | 7.43(3) | 2882 | 18.26 | 1.508 | – | – |
| 1.75 | No | No | No | 20 | 0.354 | 0.00 | 0.557 | – | 3.10 | 8.74(3) | 1756 | 18.55 | 1.702 | – | – |
| 2.00 | No | No | Yes | 25 | 1.233 | 0.50 | 0.531 | 0.616 | 2.80 | 1.03(4) | 1186 | 18.22 | 2.612 | 0.138 | 0.008 |
| 2.25 | No | No | Yes | 32 | 1.331 | 0.62 | 0.536 | 0.631 | 4.76 | 1.12(4) | 1015 | 26.79 | 2.746 | 0.114 | 0.004 |
| 2.50 | No | No | Yes | 31 | 1.744 | 0.72 | 0.546 | 0.638 | 5.22 | 1.18(4) | 770.2 | 22.40 | 2.534 | 0.294 | 0.013 |
| 2.75 | No | No | Yes | 30 | 2.421 | 0.77 | 0.567 | 0.634 | 5.48 | 1.24(4) | 587.5 | 16.89 | 2.141 | 0.459 | 0.027 |
| 3.00 | No | No | Yes | 28 | 2.700 | 0.80 | 0.598 | 0.641 | 6.30 | 1.30(4) | 453.6 | 12.19 | 1.706 | 0.604 | 0.050 |
| 3.25 | No | No | Yes | 25 | 2.999 | 0.81 | 0.644 | 0.664 | 7.77 | 1.41(4) | 355.5 | 8.703 | 1.243 | 0.627 | 0.072 |
| 3.50 | No | No | Yes | 24 | 2.576 | 0.90 | 0.691 | 0.700 | 11.9 | 1.57(4) | 282.0 | 6.384 | 0.869 | 0.473 | 0.074 |
| 4.00 | No | No | Yes | 23 | 1.939 | 0.96 | 0.797 | 0.800 | 34.8 | 2.08(4) | 192.7 | 3.899 | 0.392 | 0.168 | 0.043 |
| 4.50 | Yes | Yes | Yes | 31 | 1.287 | 0.96 | 0.847 | 0.850 | 63.5 | 2.73(4) | 141.0 | 2.607 | 0.338 | 0.028 | 0.011 |
| 5.00 | Yes | Yes | Yes | 41 | 0.844 | 0.95 | 0.863 | 0.866 | 75.4 | 3.06(4) | 108.2 | 1.996 | 0.352 | – | – |
| 5.50 | Yes | Yes | Yes | 49 | 0.854 | 0.94 | 0.883 | 0.884 | 81.4 | 3.49(4) | 85.07 | 1.558 | 0.334 | – | – |
| 6.00 | Yes | Yes | Yes | 51 | 0.894 | 0.93 | 0.905 | 0.907 | 85.5 | 3.96(4) | 69.85 | 1.160 | 0.282 | – | – |
| 7.00 | Yes | Yes | Yes | 56 | 0.769 | 0.92 | 0.962 | 0.964 | 92.4 | 4.99(4) | 48.44 | 0.709 | 0.166 | – | – |
| 8.00 | Yes | Yes | Yes | 67 | 0.570 | 0.87 | 1.052 | 1.053 | 100 | 6.37(4) | 36.52 | 0.435 | 0.086 | – | – |
| $Z = 0.03$, $Y = 0.30$ models. | | | | | | | | | | | | | | | |
| 1.00 | No | No | No | 6 | 0.478 | 0.00 | 0.580 | – | 1.76 | 3.99(3) | 16164 | 22.84 | 0.420 | – | – |
| 1.25 | No | No | No | 10 | 0.423 | 0.00 | 0.560 | – | 2.42 | 5.10(3) | 7004 | 21.86 | 0.679 | – | – |
| 1.50 | No | No | No | 14 | 0.388 | 0.00 | 0.561 | – | 2.75 | 6.26(3) | 3655 | 20.71 | 0.922 | – | – |
| 1.75 | No | No | No | 17 | 0.362 | 0.00 | 0.563 | – | 3.05 | 7.33(3) | 2183 | 18.78 | 1.119 | – | – |
| 2.00 | No | No | No | 22 | 0.355 | 0.00 | 0.559 | – | 3.37 | 8.45(3) | 1450 | 20.65 | 1.403 | – | – |
| 2.25 | No | No | No | 28 | 0.349 | 0.00 | 0.547 | – | 3.76 | 9.66(3) | 1161 | 28.12 | 1.895 | – | – |
| 2.50 | No | No | Yes | 31 | 0.359 | 0.09 | 0.551 | 0.668 | 4.27 | 1.10(4) | 914.2 | 25.85 | 1.984 | – | – |
| 2.75 | No | No | Yes | 33 | 0.523 | 0.44 | 0.564 | 0.666 | 5.09 | 1.22(4) | 695.0 | 20.83 | 1.768 | – | – |
| 3.00 | No | No | Yes | 33 | 0.911 | 0.70 | 0.580 | 0.665 | 6.20 | 1.33(4) | 532.3 | 16.79 | 1.621 | – | – |
| 3.25 | No | No | Yes | 32 | 1.307 | 0.78 | 0.611 | 0.667 | 7.91 | 1.46(4) | 417.1 | 11.83 | 1.346 | 0.141 | 0.012 |
| 3.50 | No | No | Yes | 33 | 1.523 | 0.84 | 0.646 | 0.677 | 12.7 | 1.59(4) | 327.8 | 9.610 | 1.161 | 0.254 | 0.026 |
| 3.75 | No | No | Yes | 32 | 1.497 | 0.86 | 0.687 | 0.705 | 16.0 | 1.71(4) | 264.1 | 7.522 | 0.889 | 0.246 | 0.033 |
| 4.00 | No | No | Yes | 24 | 1.226 | 0.91 | 0.741 | 0.751 | 19.0 | 1.86(4) | 219.2 | 5.197 | 0.496 | 0.060 | 0.012 |
| 4.25 | No | No | Yes | 19 | 0.894 | 0.94 | 0.790 | 0.796 | 24.4 | 2.05(4) | 182.1 | 4.108 | 0.260 | – | – |
| 4.50 | Yes | No | Yes | 20 | 0.786 | 0.93 | 0.832 | 0.836 | 31.9 | 2.26(4) | 154.8 | 3.299 | 0.189 | – | – |
| 4.75 | Yes | No | Yes | 21 | 0.838 | 0.94 | 0.843 | 0.846 | 42.6 | 2.41(4) | 132.2 | 2.668 | 0.178 | – | – |
| 5.00 | Yes | Yes | Yes | 26 | 0.885 | 0.94 | 0.851 | 0.855 | 54.2 | 2.59(4) | 115.7 | 2.306 | 0.202 | – | – |
| 5.50 | Yes | Yes | Yes | 31 | 0.733 | 0.94 | 0.869 | 0.873 | 64.7 | 2.97(4) | 90.08 | 1.662 | 0.191 | – | – |
| 6.00 | Yes | Yes | Yes | 33 | 0.604 | 0.93 | 0.891 | 0.894 | 71.2 | 3.35(4) | 72.55 | 1.218 | 0.176 | – | – |
| 7.00 | Yes | Yes | Yes | 43 | 0.349 | 0.90 | 0.948 | 0.951 | 82.7 | 4.22(4) | 50.14 | 0.708 | 0.120 | – | – |
| 8.00 | Yes | Yes | Yes | 63 | 0.290 | 0.85 | 1.041 | 1.043 | 94.0 | 5.73(4) | 36.64 | 0.434 | 0.078 | – | – |

**Table 2.** Stellar models calculated with variable helium compositions.

| Mass ($M_\odot$) | SDU | HBB | TDU | #TP | C/O$_f$ | $\lambda_{max}$ | $M_c(1)$ ($M_\odot$) | $M_c^{min}$ ($M_\odot$) | $T_{bce}^{max}$ (MK) | $L_{agb}^{max}$ ($L_\odot$) | $\tau_{stellar}$ (Myr) | $\tau_{agb}$ (Myr) | $\tau_{tpagb}$ (Myr) | $\tau_c$ (Myr) | $\tau_c/\tau_{agb}$ |
|---|---|---|---|---|---|---|---|---|---|---|---|---|---|---|---|
| $Z = 0.014$, $Y = 0.26$ models. | | | | | | | | | | | | | | | |
| 2.0 | No | No | Yes | 24 | 1.179 | 0.46 | 0.544 | 0.631 | 3.65 | 1.01(4) | 1324 | 20.88 | 2.408 | 0.061 | 0.003 |
| 2.25 | No | No | Yes | 30 | 1.436 | 0.64 | 0.529 | 0.624 | 4.42 | 1.05(4) | 1065 | 27.07 | 3.045 | 0.212 | 0.008 |
| 2.5 | No | No | Yes | 30 | 1.850 | 0.73 | 0.535 | 0.625 | 4.61 | 1.11(4) | 858.8 | 25.83 | 2.990 | 0.355 | 0.014 |
| 3.0 | No | No | Yes | 29 | 3.037 | 0.81 | 0.579 | 0.632 | 5.87 | 1.26(4) | 509.7 | 11.47 | 2.163 | 0.774 | 0.054 |
| 4.0 | No | No | Yes | 24 | 2.525 | 0.96 | 0.770 | 0.774 | 24.2 | 1.91(4) | 213.8 | 4.426 | 0.536 | 0.284 | 0.064 |
| 4.5 | Yes | Yes | Yes | 32 | 1.218 | 0.96 | 0.842 | 0.844 | 63.2 | 2.67(4) | 153.8 | 2.968 | 0.408 | 0.029 | 0.010 |
| $Z = 0.014$, $Y = 0.30$ models. | | | | | | | | | | | | | | | |
| 2.0 | No | No | Yes | 27 | 0.416 | 0.16 | 0.555 | 0.654 | 3.59 | 1.03(4) | 1101 | 19.06 | 1.882 | – | – |
| 2.25 | No | No | Yes | 33 | 1.289 | 0.64 | 0.548 | 0.655 | 4.78 | 1.20(4) | 912.9 | 23.72 | 2.322 | 0.048 | 0.002 |
| 2.5 | No | No | Yes | 32 | 1.616 | 0.69 | 0.561 | 0.653 | 5.62 | 1.26(4) | 691.4 | 18.47 | 2.093 | 0.188 | 0.010 |
| 3.0 | No | No | Yes | 26 | 2.313 | 0.79 | 0.619 | 0.657 | 6.88 | 1.38(4) | 400.6 | 10.29 | 1.289 | 0.410 | 0.040 |
| 4.0 | Yes | No | Yes | 23 | 1.750 | 0.95 | 0.826 | 0.828 | 47.6 | 2.32(4) | 173.3 | 3.277 | 0.291 | 0.108 | 0.033 |
| 4.5 | Yes | Yes | Yes | 29 | 1.206 | 0.94 | 0.854 | 0.856 | 64.1 | 2.80(4) | 127.8 | 2.364 | 0.268 | 0.024 | 0.010 |
| $Z = 0.014$, $Y = 0.35$ models. | | | | | | | | | | | | | | | |
| 2.0 | No | No | No | 27 | 0.340 | 0.00 | 0.579 | – | 3.60 | 1.11(4) | 906.9 | 16.65 | 1.283 | – | – |
| 2.25 | No | No | Yes | 30 | 0.432 | 0.21 | 0.590 | 0.686 | 4.40 | 1.26(4) | 694.3 | 14.36 | 1.239 | – | – |
| 2.5 | No | No | Yes | 31 | 1.209 | 0.60 | 0.612 | 0.680 | 5.99 | 1.43(4) | 517.7 | 11.47 | 1.095 | 0.055 | 0.005 |
| 3.0 | No | No | Yes | 24 | 1.708 | 0.79 | 0.686 | 0.711 | 12.2 | 1.64(4) | 299.8 | 6.729 | 0.589 | 0.153 | 0.023 |
| 3.5 | No | No | Yes | 22 | 1.687 | 0.94 | 0.796 | 0.802 | 30.0 | 2.16(4) | 192.6 | 3.740 | 0.266 | 0.086 | 0.023 |
| 4.0 | Yes | Yes | Yes | 23 | 1.275 | 0.93 | 0.855 | 0.859 | 50.4 | 2.57(4) | 134.1 | 2.468 | 0.159 | 0.028 | 0.011 |
| 4.5 | Yes | Yes | Yes | 30 | 1.087 | 0.92 | 0.874 | 0.877 | 66.1 | 3.02(4) | 100.3 | 1.690 | 0.162 | 0.007 | 0.004 |
| 5.0 | Yes | Yes | Yes | 38 | 0.800 | 0.91 | 0.895 | 0.899 | 78.2 | 3.46(4) | 77.37 | 1.249 | 0.157 | – | – |
| $Z = 0.014$, $Y = 0.40$ models. | | | | | | | | | | | | | | | |
| 2.0 | No | No | No | 20 | 0.323 | 0.00 | 0.632 | – | 3.60 | 1.19(4) | 706.8 | 10.23 | 0.540 | – | – |
| 2.25 | No | No | No | 24 | 0.333 | 0.00 | 0.644 | – | 4.41 | 1.36(4) | 511.1 | 9.674 | 0.575 | – | – |
| 2.5 | No | No | Yes | 22 | 0.357 | 0.13 | 0.677 | 0.729 | 5.66 | 1.52(4) | 378.4 | 7.313 | 0.427 | – | – |
| 3.0 | No | No | Yes | 17 | 0.755 | 0.56 | 0.773 | 0.787 | 12.7 | 1.93(4) | 224.7 | 4.058 | 0.169 | – | – |
| 4.0 | Yes | Yes | Yes | 26 | 0.994 | 0.80 | 0.879 | 0.884 | 53.3 | 2.80(4) | 104.5 | 1.660 | 0.101 | – | – |
| 4.5 | Yes | Yes | Yes | 34 | 0.727 | 0.79 | 0.905 | 0.912 | 69.6 | 3.36(4) | 77.85 | 1.111 | 0.092 | – | – |
| $Z = 0.03$, $Y = 0.32$ models. | | | | | | | | | | | | | | | |
| 3.0 | No | No | Yes | 31 | 0.667 | 0.60 | 0.600 | 0.674 | 6.20 | 1.37(4) | 532.3 | 16.76 | 1.585 | – | – |
| 3.5 | No | No | Yes | 28 | 1.115 | 0.81 | 0.669 | 0.698 | 11.5 | 1.61(4) | 290.8 | 8.065 | 0.761 | 0.050 | 0.006 |
| 4.0 | No | No | Yes | 19 | 0.838 | 0.87 | 0.771 | 0.779 | 19.0 | 1.94(4) | 194.2 | 4.389 | 0.269 | – | – |
| 5.0 | Yes | Yes | Yes | 25 | 0.799 | 0.92 | 0.859 | 0.863 | 55.1 | 2.67(4) | 104.1 | 2.056 | 0.160 | – | – |
| $Z = 0.03$, $Y = 0.35$ models. | | | | | | | | | | | | | | | |
| 3.0 | No | No | Yes | 28 | 0.461 | 0.39 | 0.632 | 0.697 | 6.10 | 1.44(4) | 387.0 | 10.95 | 0.783 | – | – |
| 3.25 | No | No | Yes | 23 | 0.615 | 0.58 | 0.680 | 0.713 | 7.22 | 1.48(4) | 307.0 | 6.986 | 0.465 | – | – |
| 3.5 | No | No | Yes | 21 | 0.699 | 0.72 | 0.717 | 0.736 | 11.4 | 1.72(4) | 242.3 | 6.023 | 0.341 | – | – |
| 4.0 | Yes | No | Yes | 14 | 0.521 | 0.75 | 0.822 | 0.828 | 18.9 | 2.15(4) | 163.1 | 3.463 | 0.106 | – | – |
| 4.25 | Yes | No | Yes | 18 | 0.640 | 0.85 | 0.842 | 0.848 | 24.8 | 2.34(4) | 138.1 | 2.876 | 0.118 | – | – |
| 4.5 | Yes | No | Yes | 20 | 0.632 | 0.85 | 0.852 | 0.857 | 33.3 | 2.45(4) | 118.6 | 2.317 | 0.118 | – | – |
| 4.75 | Yes | No | Yes | 24 | 0.673 | 0.86 | 0.861 | 0.867 | 44.8 | 2.61(4) | 101.9 | 1.971 | 0.126 | – | – |
| 5.0 | Yes | Yes | Yes | 27 | 0.697 | 0.88 | 0.870 | 0.875 | 56.3 | 2.80(4) | 89.68 | 1.666 | 0.130 | – | – |
| $Z = 0.03$, $Y = 0.40$ models. | | | | | | | | | | | | | | | |
| 3.0 | No | No | No | 16 | 0.349 | 0.00 | 0.713 | – | 6.00 | 1.60(4) | 283.0 | 6.141 | 0.223 | – | – |
| 3.5 | No | No | No | 13 | 0.344 | 0.00 | 0.813 | – | 10.3 | 2.09(4) | 180.9 | 3.540 | 0.080 | – | – |
| 4.0 | Yes | No | Yes | 14 | 0.384 | 0.31 | 0.855 | 0.863 | 19.7 | 2.41(4) | 123.6 | 2.356 | 0.060 | – | – |
| 5.0 | Yes | Yes | Yes | 33 | 0.537 | 0.66 | 0.894 | 0.904 | 59.2 | 3.09(4) | 68.72 | 1.242 | 0.091 | – | – |

lower mass models at $Z = 0.03$ experience considerably shallower dredge-up, with TDU only starting at $2.5M_\odot$ (compared to $2M_\odot$ at $Z = 0.014$). While the $2.5M_\odot$, $Z = 0.03$ model experiences some TDU it does not become carbon rich.

The $Z = 0.007$ models are similar in metallicity to the $Z = 0.008$ models from Karakas et al. (2002). Doherty et al. (2014) present evolution and nucleosynthesis results for a $7M_\odot$, $Z = 0.008$ model, similar to our most massive case. The minimum mass for the TDU is $1.5M_\odot$ in the $Z = 0.008$ models with mass loss, although dredge-up is shallow with a maximum $\lambda = 0.084$. This is very similar to the new $Z = 0.007$ models, where dredge-up also starts at $1.5M_\odot$, where $\lambda_{max} = 0.1$. Dredge-up is deeper

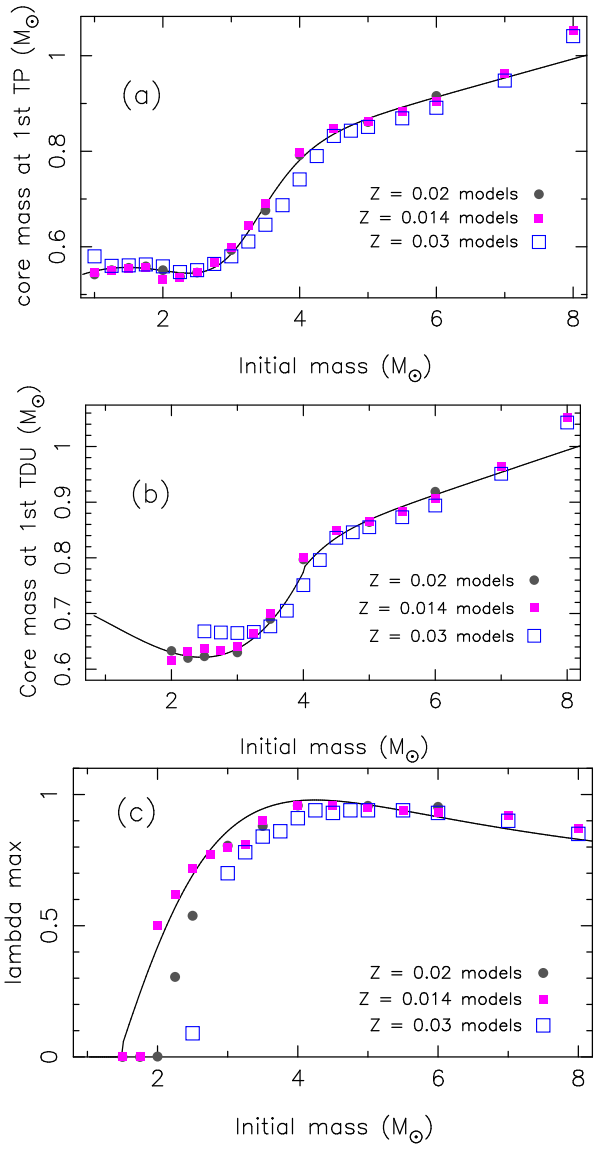


**Figure 1.** (a) The core mass at the first thermal pulse, $M_{\rm c}(1)$, (b) the core mass at the first third dredge-up episode, $M_{\rm c}^{\rm min}$, and (c) the maximum third dredge-up efficiency parameter, $\lambda_{\rm max}$ for the new $Z = 0.014$ (solid magenta squares) and $Z = 0.03$ (large open blue squares) models using data from Table 1. The fits to the $Z = 0.02$ models from Karakas et al. (2002) are shown by the solid lines, as are the model data for the $Z = 0.02$ models with mass loss (solid dark grey circles), also from Karakas et al. (2002).

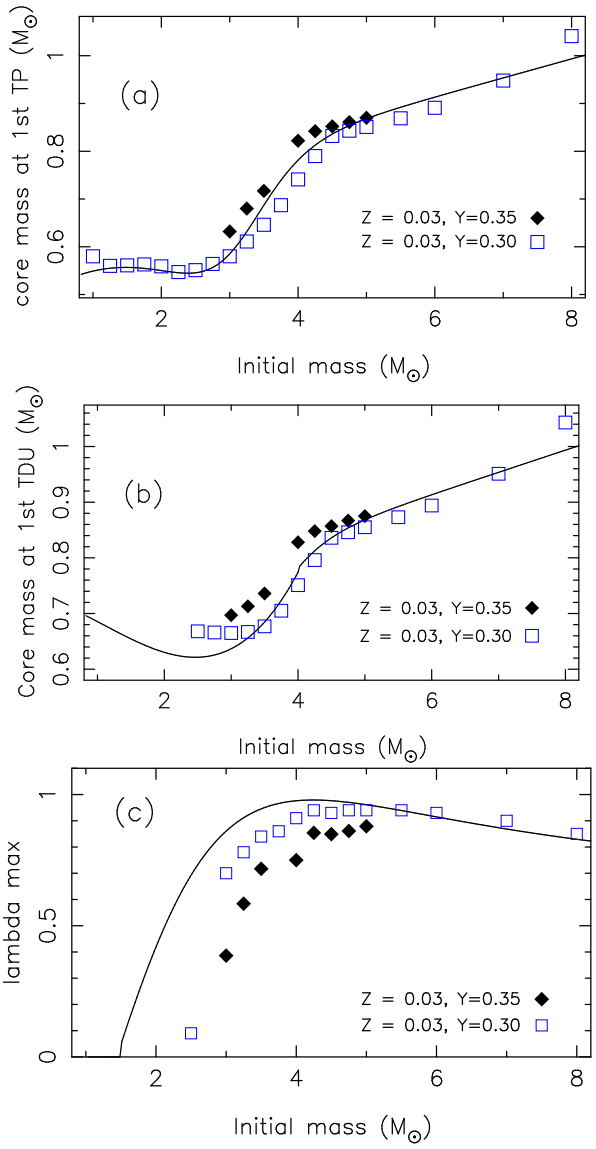


**Figure 2.** (a) The core mass at the first thermal pulse, $M_{\rm c}(1)$, (b) the core mass at the first third dredge-up episode, $M_{\rm c}^{\rm min}$, and (c) the maximum third dredge-up efficiency parameter, $\lambda_{\rm max}$ for $Z = 0.03$ models (large open blue squares) with a canonical helium abundance ($Y = 0.30$) and for $Z = 0.03$ models with $Y = 0.35$. The fits to the $Z = 0.02$ models from Karakas et al. (2002) are shown by the solid lines.

in the $Z = 0.007$ models for masses between $1.75{\rm M}_{\odot}$ and $2.5{\rm M}_{\odot}$ but after that the two model sets are similar. The minimum core masses at the first thermal pulse and first TDU are higher in the $Z = 0.007$ models. Besides the difference in metallicity, the stellar evolutionary code used for the calculations has been updated to use the LUNA rate (Bemmerer et al. 2006) for the $^{14}{\rm N(p,\gamma)}^{15}{\rm O}$ reaction, which governs the main-sequence lifetime and consequently the size of the H-exhausted core at the end. Furthermore, the code now uses the NACRE rate (Angulo et al. 1999) for the triple-$\alpha$ process and the $^{12}{\rm C}(\alpha,\gamma)^{16}{\rm O}$ reaction (instead of the rates from Caughlan & Fowler 1988), both of which govern energy generation during core He burning and therefore the size of the core at the beginning of the AGB (e.g., Castellani et al. 1992; Imbriani et al. 2001; Halabi et al. 2012).

In Figure 2 we illustrate the effect of an enhanced helium composition on the third dredge-up, where we plot the $Z = 0.03$ models with $Y = 0.35$ against the canonical helium abundance models. While we only have 8 models for comparison, it is clear that an enhanced helium abundance increases the core mass at the first thermal pulse, and therefore at the first TDU episode, and importantly, lowers the maximum third dredge-up efficiency found at a given mass. From Table 2 we can see similar behaviour in the helium-enhanced $Z = 0.014$ models. The reduction in $\lambda$ is most

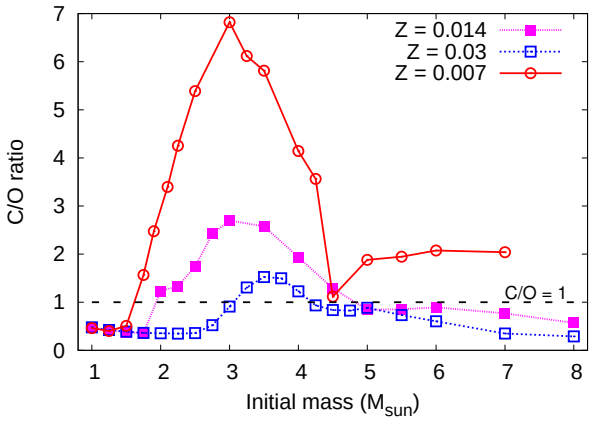


**Figure 3.** The final C/O ratio at the surface as a function of initial stellar mass for the stellar models in Table 1.

apparent at the lowest masses that experience TDU, which has important consequences for the production of carbon stars in metal-rich populations.

Increasing the helium content changes the mean molecular weight, $\mu$, which results in hotter H-burning regions and higher luminosities. As a consequence, the whole star is bigger, brighter and has a lower effective temperature (a consequence of a larger radius). This means that the mass-loss rate is higher, which in turn reduces the number of TPs as can be seen most noticeably for the $Y = 0.40$ models in Table 2. In the metal-rich models of $Z = 0.03$, TDU does not begin until e.g., the 11th TP in the 3.5M$_\odot$ model with $Y = 0.30$. The same model of $Y = 0.40$ only has 12TP and by the 11th the total mass has been reduced by $\approx 1$M$_\odot$. This reduction in number of TPs may be the main reason for the reduction in $\lambda_{\rm max}$ (which has been shown to increase steadily with thermal pulse in lower mass stars, e.g., Karakas et al. 2002).

### 3.2 The C/O ratio

In Figure 3 we show the range of final C/O ratios predicted from the canonical stellar evolutionary sequences. All $Z = 0.007$ models more massive than 1.5M$_\odot$ become C-rich by the tip of the AGB, including the intermediate-mass AGB stars that suffer HBB. The final C/O ratio does not reflect the evolution of the C/O ratio for HBB models, which spend the majority of the TP-AGB with C/O $< 1$ as a consequence of efficient envelope burning. As an example, the 6M$_\odot$, $Z = 0.007$ model experiences 64 TPs and only becomes C-rich after the 62nd, from Table 1 we see that the C-rich phase lasts for about 2% of the entire AGB phase. At higher metallicities dredge-up also occurs but there is less oxygen depletion by HBB (and the initial O abundance is much higher) which means that the models do not become C-rich.

Lower mass stars that do not experience HBB can have C-rich lifetimes that are $\gtrsim 10\%$ of the total AGB lifetime in the lowest metallicity models (Table 1). The ratio of the C-rich lifetime to the total AGB lifetime can be used as a proxy for the ratio of the number of C stars to O-rich M-type AGB stars, C/M, in a given population. In the metal-rich models of $Z = 0.03$ this ratio has a maximum of $\approx 0.03$ at 3.75M$_\odot$, whereas it reaches much higher values of $\approx 0.07$ in solar metallicity models. Increasing the helium content of the model greatly reduces the number of carbon stars, where Table 2 shows that an increase of $\Delta Y = 0.07$ at solar metallicity reduces the ratio to 0.02. In the metal-rich models an increase of helium almost entirely wipes out the C-star population.

Figure 3 illustrates that the mass range of carbon-stars is predicted to shrink with an increase in the metallicity. By the time we get to $Z = 0.03$ only a narrow mass range between 3.25M$_\odot$ to 4M$_\odot$ become carbon rich, compared to 2M$_\odot$ to 4.5M$_\odot$ at $Z = 0.014$. Furthermore, the maximum C/O ratio also decreases with increasing metallicity as a consequence of a higher initial oxygen abundance. Models with masses near 5M$_\odot$ at $Z = 0.014$ and $Z = 0.03$ experience mild HBB. It is enough to keep the C/O ratio less than unity but Figure 3 shows that the final C/O ratio is $\approx 0.9$. One or more TDU episode (at the same efficiency) would be enough for the model to become C-rich.

All intermediate-mass stars experienced convergence problems of the type discussed by Lau et al. (2012) and the models terminated with reasonably large envelope masses ($\approx 1$M$_\odot$). This means that the lifetimes given in Tables 1 and 2 are lower limits although in Karakas et al. (2014) we estimated that one or two missed TPs is not going to affect the total stellar lifetimes or AGB lifetimes of models with $M \lesssim 2.4$M$_\odot$. For intermediate-mass AGB stars, we may be missing up to 3 or more TPs. As an example, we estimate that the 5M$_\odot$, $Z = 0.03$ model may experience another 3 TPs, which would increase the AGB lifetime by $\approx 33,000$ years (taking a maximum interpulse period of 11,000 years). This is a negligible increase to the total and AGB lifetimes but increases the TP-AGB phase by about 16%.

In Figure 4 we show the final C/O ratios for the stellar models calculated with different helium compositions. We draw a line through the points with $Y = 0.35$ to highlight how the C/O ratio decreases in helium-rich AGB models. The main point to take away from this diagram is that an increase in helium by only $\Delta Y = 0.05$ is enough to inhibit carbon star production altogether at $Z = 0.03$. Models that experience the largest shift toward lower C/O ratios are those at the minimum mass for the onset of the TDU, that is, stars with $M \approx 2 - 3$M$_\odot$ according to our models.

### 3.3 Comparison to other studies

While there are no other $Z = 0.03$ AGB models for comparison, we can compare the solar and $Z = 0.007$ models to other studies. Here we compare to the 2M$_\odot$, $Z = 0.0138$ model from Cristallo et al. (2009) and to the 3M$_\odot$, $Z = 0.02$ model from Cristallo et al. (2011, noting that evolution model data is not available in the paper for the 3M$_\odot$, $Z = 0.0138$ model). We also provide a comparison between our most massive AGB model of 7M$_\odot$, $Z = 0.007$ to the calculations by Ventura et al. (2013), which use the Full Spectrum of Turbulence convective prescription. While there are other AGB models for comparison, including the intermediate-mass and super-AGB AGB models by Doherty et al. (2014) and the MESA models by Pignatari et al. (2013), we limit our comparison for the sake of brevity.

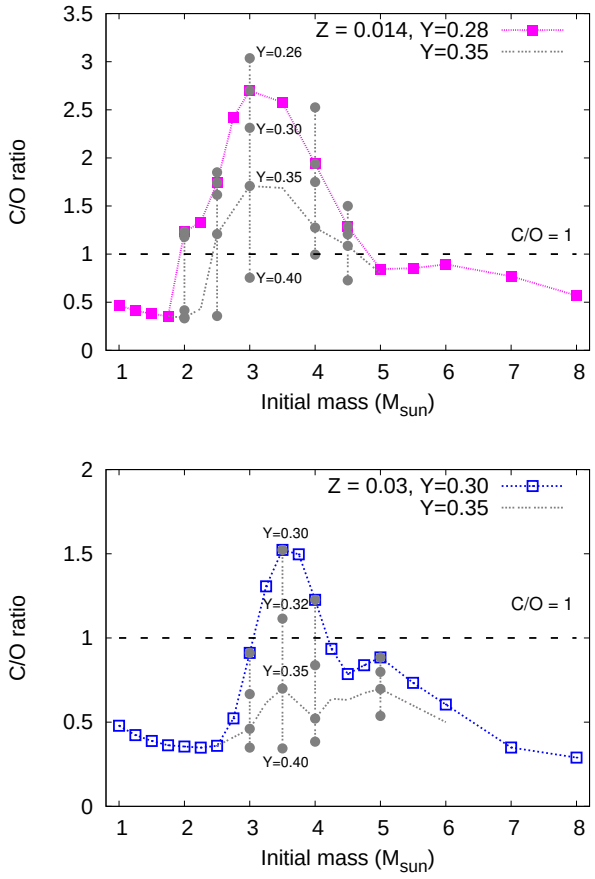


**Figure 4.** The final C/O ratio for the (a) $Z = 0.014$ models, including the models with a helium compositions between $Y = 0.26$ to $Y = 0.40$, and (b) the $Z = 0.03$ models, including models with helium compositions between $Y = 0.32$ to $Y = 0.40$.

Our $2M_{\odot}$, $Z = 0.014$ model becomes carbon rich, with a final C/O = 1.23 and dredges up a total of $0.0236M_{\odot}$ over 25 TPs during the TP-AGB. In comparison, the $2M_{\odot}$, $Z = 0.0138$ model from Cristallo et al. (2009) experiences 12 TPs during the AGB and dredges up a total of $0.0362M_{\odot}$, with a final C/O=1.88. The model by Cristallo et al. also becomes C-rich at a lower core mass of $0.603M_{\odot}$ compared to our $0.65M_{\odot}$ (and presumably at a lower luminosity, although this is not included in their tables).

The model by Cristallo et al. (2009) has convective boundary mixing included, through the use of an exponentially-decaying diffusive overshoot scheme dependent on the parameter $\beta$, which is similar to the scheme adopted by Herwig (2000). While our model has no formal mixing beyond the Schwarzschild border, we adopt the search for a neutral border to the convective-radiative boundary described by Lattanzio (1986) which has been found to increase the amount of TDU relative to schemes that strictly adopt the Schwarzschild criterion (Frost & Lattanzio 1996). Adopting the mixing scheme used by Cristallo et al. (2009) with their choice of $\beta$, leads to deeper TDU at a much lower core mass than we find in our calculation (see also discussion in Herwig 2000). We would need to include such a mixing scheme if we were to try and reproduce the Galactic C-star luminosity function, which peaks at a bolometric luminosity of about −4.9, where there are very few Galactic C-stars with luminosities higher than this (Whitelock et al. 2006; Guandalini et al. 2006; Guandalini & Cristallo 2013).

We can include convective overshoot in a simple manner by extending the base of the convective envelope by $N$ pressure scale heights, as done by Karakas, Campbell, & Stancliffe (2010). If we set $N = 2$, we can calculate a $2M_{\odot}$, $Z = 0.014$ AGB model with similar characteristics to the model by Cristallo et al. (2009). The minimum core mass for TDU is reduced from $0.616M_{\odot}$ with no overshoot to $0.577M_{\odot}$, which is similar although still slightly higher than the minimum core mass for TDU of $0.568M_{\odot}$ found by Cristallo et al. (2009).

We now compare the $3M_{\odot}$, $Z = 0.014$ model to the $3M_{\odot}$, $Z = 0.02$ model by Cristallo et al. (2011). The $3M_{\odot}$ model by Cristallo et al. enters the AGB at a much higher core mass of $0.653M_{\odot}$ and becomes C-rich at a core mass of $0.677M_{\odot}$. The final core mass is $0.700M_{\odot}$. In comparison, the slightly lower metallicity Stromlo model enters the AGB at a core mass of $0.598M_{\odot}$, becomes C-rich at $0.669M_{\odot}$ and has a final core mass of $0.691M_{\odot}$. The Stromlo model experiences 28 TP, and has a final C/O=2.7, and dredges up $0.1M_{\odot}$ from the He-shell. In comparison, the Cristallo et al. model has 14 TPs, a final C/O=1.59, and dredges up $0.0754M_{\odot}$. The C-rich lifetime of the Cristallo et al. (2011) model is shorter, at 0.462 Myr relative to our 0.604 Myr. Increasing the mass-loss rate on the AGB in our calculation would reduce the difference in final C/O and C-rich lifetimes. In summary, the Cristallo et al. model has a higher core mass and presumably a higher luminosity, although within the range of uncertainties in stellar models the results are reasonably consistent.

While both the current set of models and models by Cristallo et al. (2011) predict the occurrence of carbon stars with masses above $2M_{\odot}$, we emphasise that C-stars evolving from such progenitor stars will be very rare in stellar populations for the following reasons: 1) the initial mass function favours stars of lower mass, and 2) because they have short AGB and C-rich lifetimes.

We now compare the $7M_{\odot}$, $Z = 0.007$ model to the $7M_{\odot}$, $Z = 0.008$ model by Ventura et al. (2013). This model was calculated with the Full Spectrum of Turbulence convective prescription which results in a stronger HBB during the AGB (Ventura & D'Antona 2005a). This means that the peak HBB temperature is higher, at 105 MK, than the Stromlo model which peaks at 103 MK (noting that the Stromlo model has a lower metallicity, which also results in higher temperatures). The Stromlo model becomes C-rich at the very tip of the AGB, has a final helium mass fraction at the surface of $Y = 0.352$, and experiences 61 TPs. The final core mass is $1.04M_{\odot}$. In comparison, the $7M_{\odot}$ model by Ventura et al. only has 24 TP, destroys considerable carbon such that the final C/O is well below unity, has a final surface $Y = 0.36$, and a final core mass of $1.14M_{\odot}$.

The $7M_{\odot}$ Stromlo model becomes carbon rich because TDU continues after the cessation of HBB, which allows the C abundance to increase (Frost et al. 1998). van Loon et al. (1999) presented observational evidence that supports this scenario, finding a sample of very luminous, dust-obscured C-rich AGB stars in the Magellanic Clouds. The existence

of very bright, C-rich AGB stars is also evidence that stars in this mass range experience TDU at the metallicities of the Magellanic Clouds.

## 4 MODELLING UNCERTAINTIES

The evolution and nucleosynthesis of low-mass and intermediate-mass stars is significantly affected by numerical modelling uncertainties as well as uncertainties in the input physics (see Karakas & Lattanzio 2014, for a detailed discussion). The main uncertainties affecting the current study are the treatment of convection and in particular, the numerical treatment of convective borders and the mass-loss rate used on the AGB (e.g., Ventura & D'Antona 2005a,b; Stancliffe & Jeffery 2007; Cristallo et al. 2009). The method for determining convective borders in particular determines the occurrence of the TDU (Frost & Lattanzio 1996; Mowlavi 1999), and the minimum initial stellar mass for carbon-star production, while the mass-loss rate determines the number of thermal pulses and the AGB lifetime (Blöcker 1995).

For models near the minimum mass for the onset of the TDU, dredge-up becomes less efficient as the metallicity increases. The treatment of convection and of convective borders is of paramount importance here. Convective boundary mixing as applied by e.g, Herwig (2000), will decrease the minimum mass for carbon star production to whatever mass one desires. However, observations of C stars in the Galaxy are hindered by uncertain distances which means that the minimum mass from observations is not well constrained (Wallerstein & Knapp 1998), although can be inferred from carbon-star luminosity functions to be $\approx 1.5 M_{\odot}$ (e.g., Whitelock et al. 2006; Guandalini et al. 2006; Guandalini & Cristallo 2013).

Guandalini & Cristallo (2013) re-derived the C-star luminosity function for Galactic C stars and find good agreement with the theoretical C-star luminosity function from Cristallo et al. (2011), which has a minimum C-star mass of $1.5 M_{\odot}$ at solar metallicity. As described earlier, the models by Cristallo et al. (2011) employ a convective boundary mixing scheme, which requires a free parameter in order to obtain dredge-up at the lowest masses. We require a considerable amount of convective overshoot (3 pressure scale heights) for the $1.5 M_{\odot}$, $Z = 0.014$ model to become C-rich. While large, this is similar to the amount of overshoot Kamath et al. (2012) required in order to get the correct O-rich to C-rich transition luminosity in lower metallicity Magellanic Cloud clusters. Note that a similar amount of overshoot lowers the minimum mass for C-star production from $3.25 M_{\odot}$ at $Z = 0.03$ to $2.5 M_{\odot}$.

The models by Cristallo et al. (2011) and Ventura et al. (2013) experience many fewer TPs than the calculations presented here. While the convective prescription in the envelope plays a more dominant role in intermediate-mass models (Ventura & D'Antona 2005a), in lower-mass models the mass-loss rate on the AGB is crucial. We use the Vassiliadis & Wood (1993) semi-empirical prescription, which was derived from a sample of Galactic and Magellanic Cloud O and C-rich AGB stars. The mass-loss rate used by Cristallo et al. (2009) is based on a similar semi-empirical calibration to Vassiliadis & Wood (1993) of the period-mass loss relations of long-period variables (Straniero et al. 2006).

Star clusters in the Galaxy can be used to probe uncertain physics in stellar evolutionary calculations such as mass loss and convection (Weidemann 2000; Marigo 2001; Ferrario et al. 2005; Kalirai et al. 2008, 2009; Cristallo et al. 2011). The core mass at the first thermal pulse is a good estimate of the final mass for stars more massive than about $4 M_{\odot}$, which only experience shallow core growth owing to efficient TDU and short interpulse periods during which the H-burning shell is dominant. For stars less massive than about $4 M_{\odot}$, the core growth is more significant and is determined by the depth of TDU and the mass-loss rate, which determines the AGB lifetime and hence the amount of core growth (e.g., Kalirai et al. 2014).

Kalirai et al. (2007) determined the initial masses of the white dwarfs ($0.61 \pm 0.02 M_{\odot}$) in the solar metallicity cluster NGC 7789 to be $2.02 \pm 0.07 M_{\odot}$. Our $2 M_{\odot}$, $Z = 0.014$ model has a final mass of $0.659 M_{\odot}$. In order to reproduce a final mass of $0.61 M_{\odot}$, we require convective overshoot on the order of 2 pressure scale heights from the formal border. Again, this is consistent with previous studies and suggests that convective boundary mixing occurs in such stars.

The cluster NGC 6791 has a metallicity of [Fe/H] = +0.4, similar to our $Z = 0.03$ models. However, our $1 M_{\odot}$, $Z = 0.03$ produces a final core mass of $0.57 M_{\odot}$, larger than the mass of the white dwarfs in this cluster, at $0.53 M_{\odot}$ (Kalirai et al. 2008). At such low initial masses, the TDU is not predicted to occur so the uncertain details of He-burning determine the size of the core on the AGB (see discussion in Karakas & Lattanzio 2014). Mass loss on the RGB is also important, as discussed by Kalirai et al. (2007). Helium enrichment increases the core masses of the models at the start of the AGB, which implies that it is unlikely that any of the cluster member stars are strongly helium rich.

Kalirai et al. (2014) compared the core mass growth from theoretical calculations using different mass-loss prescriptions to the white dwarf masses in Galactic open clusters of solar and super-solar metallicity. These authors found that the Vassiliadis & Wood (1993) prescription agrees very well with the observational data, at least for AGB stars up to about $2 M_{\odot}$. In comparison, comparisons between the observational data and results using the Blöcker (1995) rate with $\eta = 0.2$ and the van Loon et al. (2005) rates were not so favourable.

For masses above $2 M_{\odot}$, it becomes harder to constrain the mass-loss rates of AGB stars because of the paucity of observational data. A comparison between our $3 M_{\odot}$, $Z = 0.014$ model to a similar metallicity calculation by Cristallo et al. (2011) suggests that the Vassiliadis & Wood (1993) mass-loss formula is too low at these masses. Ventura et al. (2000) calibrated the Blöcker (1995) rate against the lithium-rich, O-rich AGB stars in the Magellanic Clouds and determined a value of $\eta = 0.01$.

We test the Blöcker (1995) rate with $\eta = 0.01$ in a $3 M_{\odot}$, $Z = 0.03$, $Y = 0.30$ model and obtain a much lower mass loss relative to the Vassiliadis & Wood (1993) prescription. The $3 M_{\odot}$, $Z = 0.03$ model now has 47 TPs relative to 33, and becomes C-rich, with a final C/O = 1.7 whereas with Vassiliadis & Wood (1993) the model does not become C-rich. We find that the Blöcker (1995) mass-loss

rate with $\eta = 0.03$ results in a similar number of TPs to the Vassiliadis & Wood (1993) mass-loss rate at $3M_{\odot}$, $Z = 0.03$. Setting $\eta = 0.1$ results in a mass-loss rate that is so fast that all the envelope is lost before TDU begins. Setting $\eta = 0.01$ in a $3M_{\odot}$, $Z = 0.03$ model with $Y = 0.35$ results in the formation of C star, where the final C/O=1.35. This indicates that the amount of helium needed to remove carbon stars from a population is dependent on the mass-loss rate.

The initial solar abundances adopted are not a significant uncertainty on the stellar evolutionary calculations of solar metallicity. This is demonstrated by the reasonably good agreement between the $Z = 0.014$ models presented here and the previous $Z = 0.02$ models. To test this assumption further, we adopt the solar abundances by Lodders et al. (2009), which have a proto-solar metallicity of $Z = 0.0153$, in a model of $3M_{\odot}$. The $3M_{\odot}$, $Z = 0.0153$ model has very similar characteristics to the model of $Z = 0.014$: 29 TPs instead of 28, $0.091M_{\odot}$ of material dredged up relative to $0.1M_{\odot}$, and the same tip AGB luminosity of $13,000L_{\odot}$.

Finally, we comment on other uncertainties that affect models of low and intermediate-mass stars including non-convective extra mixing and stellar rotation. While non-convective extra mixing on the RGB seems ubiquitous in all low-mass stars below $2M_{\odot}$ (e.g., Gilroy 1989; Eggleton et al. 2008; Charbonnel & Lagarde 2010), extra mixing on the AGB is much less certain (Busso et al. 2010; Karakas et al. 2010). By extra mixing in this context, we are referring to the mixing between the base of the convective envelope and hydrogen shell, such that the products of H-burning are observed at the surface.

The mechanism(s) responsible for mixing material from the base of the convective envelope through a hot region near the H-shell is unknown. Various mechanisms have been proposed including including thermohaline mixing (described below), magnetic buoyancy (Nordhaus et al. 2008; Nucci & Busso 2014), and stellar rotation (Herwig et al. 2003; Piersanti et al. 2013). Rotation can generally be ruled out for RGB stars (e.g., Palacios et al. 2006; Charbonnel & Lagarde 2010), although it can produce changes to AGB nucleosynthesis (Herwig et al. 2003; Piersanti et al. 2013). From the models of Piersanti et al. (2013), rotation does not appear to limit the production of C-stars at a given mass at solar metallicity although it does reduce the final [C/Fe] at the surface.

Thermohaline mixing or "double-diffusive mixing" has been shown to be effective on the RGB (Charbonnel & Zahn 2007; Eggleton et al. 2008; Denissenkov 2010; Angelou et al. 2012) but less so on the AGB (Stancliffe et al. 2009; Stancliffe 2010). Thermohaline mixing has been coupled with magnetic fields (Denissenkov et al. 2009) and with rotation (Lagarde et al. 2011).

The main effect of extra mixing is to lower the $^{12}C/^{13}C$ ratio, with only small changes to the C/O ratio. For example, Lederer et al. (2009) observed C/O=0.2 in unevolved AGB stars in the LMC cluster NGC 1978, about 0.1 below the predicted C/O=0.30. Extra mixing does not appear to be operating in the C-rich AGB stars in NGC 1978 but it does appear to be moderately efficient in the AGB envelope of the LMC cluster NGC 1846, which has a similar metallicity to NGC 1978 (Lebzelter et al. 2008). The operation of extra mixing in low-mass AGB stars does not change their C-rich status, but instead acts to lower their $^{12}C/^{13}C$ ratios relative to models without extra mixing.

## 5 CONCLUSIONS

We present grids of new stellar evolutionary models with masses between $1M_{\odot}$ to 7-$8M_{\odot}$ at metallicities of $Z = 0.007$, 0.014, and 0.03. These metallicities are appropriate for comparison to AGB and PNe populations in the disc and bulge of the Milky Way Galaxy and external galaxies such as M31 and the LMC. In a future study, we will calculate detailed nucleosynthesis predictions from these models in order to produce stellar yields and for comparison to the abundances of observed objects.

The $Z = 0.03$ models are the first detailed AGB models of this metallicity in the literature. We compare our results to the parameterization of the TDU by Karakas et al. (2002) for AGB models of $Z = 0.02$. These fits were made to models without mass loss and were calculated with a higher initial helium composition of $Y = 0.2928$. The $Z = 0.02$ models with mass loss experience shallower dredge-up than we find in the $Z = 0.014$ models with $Y = 0.28$ but are much closer to what we find for the $Z = 0.014$ models with $Y = 0.30$.

The behaviour of the TDU in the canonical $Z = 0.014$ models is well approximated by the parameterization for $Z = 0.02$ by Karakas et al. (2002). In contrast, the $Z = 0.03$ models experience considerably shallower dredge-up for $M < 4M_{\odot}$ compared to the solar metallicity models. The mass range that produces carbon stars is 1.75–$7M_{\odot}$ at $Z = 0.007$, 2–$4.5M_{\odot}$ at $Z = 0.014$, which is reduced to 3.25–$4M_{\odot}$ at $Z = 0.03$. The $3M_{\odot}$, $Z = 0.03$ model almost becomes C-rich, where the final C/O = 0.91. We have discussed how uncertain input physics such as the AGB mass-loss rate and the treatment of the border between convective and radiative regions will impact the calculations. Other uncertainties such as the molecular opacities (e.g., Marigo 2002) can also have a considerable impact on AGB lifetimes and will shift the minimum mass for C-star production.

In this study we also present the first helium-rich stellar evolutionary models at a solar and super-solar metallicity. We find that the third dredge-up is either reduced or inhibited when the initial helium content of the model is increased. This is caused by a reduced number of thermal pulses on the AGB relative to the canonical models. A small increase of $\Delta Y = 0.05$ is enough to inhibit carbon star production altogether at $Z = 0.03$, depending on the choice of mass-loss rate, whereas at solar metallicity we require a much larger helium enrichment of $\Delta Y \approx 0.1$ to prevent the formation of carbon stars. The consequences of removing carbon stars from super-solar metallicities on the chemical evolution of galaxies still needs to be explored, once stellar yields from such models become available.

In the inner region of M31, Boyer et al. (2013) found a very low number of carbon stars compared to the fit through observations from nearby galaxies covering a range of metallicities. The fit suggest there should be a much higher C/M star fraction at [M/H] $\approx 0.1 \pm 0.1$ (their Figure 1). The fit is also consistent with model predictions for close to solar metallicity such as those presented here, which suggests that there should be a reasonable number of carbon stars in the inner region of M31. Indeed, if anything we are un-

derestimating the number of carbon stars because we only find substantial dredge-up for $M \geqslant 2M_{\odot}$. The lack of C-stars is not simply because Boyer et al. (2013) are sampling an older population, where optical colour-magnitude diagrams for their region reveal the presence of stellar populations with a turn-off age younger than $\approx 1$ Gyr (Boyer et al. 2013). We conclude instead that the lack of carbon stars in the inner region of M31 is either the result of the metallicity being higher than estimated, at [Fe/H] $\approx 0.3$ instead of 0.1, and/or there is a substantial enrichment in helium in the observed stellar population. We show in Table 2 that an increase of $\Delta Y \approx 0.1$ at solar metallicity removes all of the carbon stars from the population.

Finally, helium appears to be an important third parameter governing the evolution and nucleosynthesis of low and intermediate-mass AGB stars. We have shown that helium is as important for the evolution of AGB stars at solar and super-solar metallicities as it is in low metallicity AGB stars (Karakas et al. 2014). We speculate that it may be possible to take the ratio of C/M stars observed in e.g., M31 by Boyer et al. (2013) and infer the level of helium enrichment in the inner regions of galaxies if the metallicity is well determined. Strong levels of helium enrichment reduce or completely remove carbon stars from populations. Estimating helium abundances from C/M star ratios would certainly be a novel way to infer the chemical enrichment of galaxies.

## ACKNOWLEDGMENTS

The author thanks the anonymous referee for comments that have improved the manuscript. The author also thanks Melissa Ness and David Nataf for comments on the manuscript, and Henry Poetrodjojo for calculating a two of the helium-rich stellar evolutionary models used for this study. AIK was supported through an Australian Research Council Future Fellowship (FT110100475).

## REFERENCES

Angelou, G. C., Stancliffe, R. J., Church, R. P., Lattanzio, J. C., & Smith, G. H. 2012, ApJ, 749, 128
Angulo, C., Arnould, M., Rayet, M., Descouvemont, P., Baye, D., Leclercq-Willain, C., Coc, A., Barhoumi, S., Aguer, P., Rolfs, C., Kunz, R., Hammer, J. W., Mayer, A., Paradellis, T., Kossionides, S., & Chronidou, C. 1999, Nucl. Phys. A, 656, 3
Asplund, M., Grevesse, N., Sauval, A. J., & Scott, P. 2009, ARA&A, 47, 481
Atlee, D. W., Assef, R. J., & Kochanek, C. S. 2009, ApJ, 694, 1539
Aver, E., Olive, K. A., Porter, R. L., & Skillman, E. D. 2013, JCAP, 11, 17
Babusiaux, C., Gómez, A., Hill, V., Royer, F., Zoccali, M., Arenou, F., Fux, R., Lecureur, A., Schultheis, M., Barbuy, B., Minniti, D., & Ortolani, S. 2010, A&A, 519, A77
Balser, D. S. 2006, AJ, 132, 2326
Bemmerer, D., Confortola, F., Lemut, A., Bonetti, R., Broggini, C., Corvisiero, P., Costantini, H., Cruz, J., Formicola, A., Fülöp, Z., Gervino, G., Guglielmetti, A., & Gustavino, C. 2006, Nuclear Physics A, 779, 297
Bensby, T., Feltzing, S., & Oey, M. S. 2014, A&A, 562, A71
Bensby, T., Yee, J. C., Feltzing, S., Johnson, J. A., Gould, A., Cohen, J. G., Asplund, M., Meléndez, J., Lucatello, S., Han, C., Thompson, I., Gal-Yam, A., Udalski, A., Bennett, D. P., Bond, I. A., Kohei, W., Sumi, T., Suzuki, D., Suzuki, K., Takino, S., Tristram, P., Yamai, N., & Yonehara, A. 2013, A&A, 549, A147
Blöcker, T. 1995, A&A, 297, 727
Boothroyd, A. I. & Sackmann, I.-J. 1988, ApJ, 328, 653
Boothroyd, A. I., Sackmann, I.-J., & Ahern, S. C. 1993, ApJ, 416, 762
Boyer, M. L., Girardi, L., Marigo, P., Williams, B. F., Aringer, B., Nowotny, W., Rosenfield, P., Dorman, C. E., Guhathakurta, P., Dalcanton, J. J., Melbourne, J. L., Olsen, K. A. G., & Weisz, D. R. 2013, ApJ, 774, 83
Brown, T. M., Sahu, K., Anderson, J., Tumlinson, J., Valenti, J. A., Smith, E., Jeffery, E. J., Renzini, A., Zoccali, M., Ferguson, H. C., VandenBerg, D. A., Bond, H. E., Casertano, S., Valenti, E., Minniti, D., Livio, M., & Panagia, N. 2010, ApJ, 725, L19
Buell, J. F. 2013, MNRAS, 428, 2577
Busso, M., Gallino, R., & Wasserburg, G. J. 1999, ARA&A, 37, 239
Busso, M., Palmerini, S., Maiorca, E., Cristallo, S., Straniero, O., Abia, C., Gallino, R., & La Cognata, M. 2010, ApJ, 717, L47
Casagrande, L., Flynn, C., Portinari, L., Girardi, L., & Jimenez, R. 2007, MNRAS, 382, 1516
Casagrande, L., Schönrich, R., Asplund, M., Cassisi, S., Ramírez, I., Meléndez, J., Bensby, T., & Feltzing, S. 2011, A&A, 530, A138
Castellani, V., Chieffi, A., & Straniero, O. 1992, ApJS, 78, 517
Caughlan, G. R. & Fowler, W. A. 1988, Atomic Data and Nuclear Data Tables, 40, 283
Charbonnel, C. & Lagarde, N. 2010, A&A, 522, A10
Charbonnel, C. & Zahn, J.-P. 2007, A&A, 467, L15
Chiappini, C., Renda, A., & Matteucci, F. 2002, A&A, 395, 789
Chung, C., Yoon, S.-J., & Lee, Y.-W. 2011, ApJ, 740, L45
Cole, A. A., Tolstoy, E., Gallagher, III, J. S., & Smecker-Hane, T. A. 2005, AJ, 129, 1465
Cole, A. A. & Weinberg, M. D. 2002, ApJ, 574, L43
Cristallo, S., Piersanti, L., Straniero, O., Gallino, R., Domínguez, I., Abia, C., Di Rico, G., Quintini, M., & Bisterzo, S. 2011, ApJS, 197, 17
Cristallo, S., Straniero, O., Gallino, R., Piersanti, L., Domínguez, I., & Lederer, M. T. 2009, ApJ, 696, 797
D'Antona, F., Bellazzini, M., Caloi, V., Pecci, F. F., Galleti, S., & Rood, R. T. 2005, ApJ, 631, 868
Denissenkov, P. A. 2010, ApJ, 723, 563
Denissenkov, P. A., Pinsonneault, M., & MacGregor, K. B. 2009, ApJ, 696, 1823
D'Ercole, A., D'Antona, F., Carini, R., Vesperini, E., & Ventura, P. 2012, MNRAS, 423, 1521
Doherty, C. L., Gil-Pons, P., Lau, H. H. B., Lattanzio, J. C., & Siess, L. 2014, MNRAS, 437, 195
Doherty, C. L., Siess, L., Lattanzio, J. C., & Gil-Pons, P. 2010, MNRAS, 401, 1453

Edvardsson, B., Andersen, J., Gustafsson, B., Lambert, D. L., Nissen, P. E., & Tomkin, J. 1993, A&A, 275, 101
Eggleton, P. P., Dearborn, D. S. P., & Lattanzio, J. C. 2008, ApJ, 677, 581
Ekström, S., Georgy, C., Eggenberger, P., Meynet, G., Mowlavi, N., Wyttenbach, A., Granada, A., Decressin, T., Hirschi, R., Frischknecht, U., Charbonnel, C., & Maeder, A. 2012, A&A, 537, A146
Ferrario, L., Wickramasinghe, D., Liebert, J., & Williams, K. A. 2005, MNRAS, 361, 1131
Frost, C. A., Cannon, R. C., Lattanzio, J. C., Wood, P. R., & Forestini, M. 1998, A&A, 332, L17
Frost, C. A. & Lattanzio, J. C. 1996, ApJ, 473, 383
García-Hernández, D. A. & Górny, S. K. 2014, A&A, 567, A12
Gennaro, M., Prada Moroni, P. G., & Degl'Innocenti, S. 2010, A&A, 518, A13
Gilroy, K. K. 1989, ApJ, 347, 835
Gonzalez, O. A., Rejkuba, M., Zoccali, M., Hill, V., Battaglia, G., Babusiaux, C., Minniti, D., Barbuy, B., Alves-Brito, A., Renzini, A., Gomez, A., & Ortolani, S. 2011, A&A, 530, A54
Górny, S. K., Perea-Calderón, J. V., García-Hernández, D. A., García-Lario, P., & Szczerba, R. 2010, A&A, 516, A39
Górny, S. K., Stasińska, G., Escudero, A. V., & Costa, R. D. D. 2004, A&A, 427, 231
Groenewegen, M. A. T. & Blommaert, J. A. D. L. 2005, A&A, 443, 143
Guandalini, R., Busso, M., Ciprini, S., Silvestro, G., & Persi, P. 2006, A&A, 445, 1069
Guandalini, R. & Cristallo, S. 2013, A&A, 555, A120
Guzman-Ramirez, L., Zijlstra, A. A., Níchuimín, R., Gesicki, K., Lagadec, E., Millar, T. J., & Woods, P. M. 2011, MNRAS, 414, 1667
Halabi, G. M., El Eid, M. F., & Champagne, A. 2012, ApJ, 761, 10
Herwig, F. 2000, A&A, 360, 952
—. 2005, ARA&A, 43, 435
Herwig, F., Langer, N., & Lugaro, M. 2003, ApJ, 593, 1056
Hill, V., Lecureur, A., Gómez, A., Zoccali, M., Schultheis, M., Babusiaux, C., Royer, F., Barbuy, B., Arenou, F., Minniti, D., & Ortolani, S. 2011, A&A, 534, A80
Imbriani, G., Limongi, M., Gialanella, L., Terrasi, F., Straniero, O., & Chieffi, A. 2001, ApJ, 558, 903
Izotov, Y. I., Thuan, T. X., & Stasińska, G. 2007, ApJ, 662, 15
Izzard, R. G., Tout, C. A., Karakas, A. I., & Pols, O. R. 2004, MNRAS, 350, 407
Johnson, C. I., Rich, R. M., Fulbright, J. P., Valenti, E., & McWilliam, A. 2011, ApJ, 732, 108
Joo, S.-J. & Lee, Y.-W. 2013, ApJ, 762, 36
Kalirai, J. S., Bergeron, P., Hansen, B. M. S., Kelson, D. D., Reitzel, D. B., Rich, R. M., & Richer, H. B. 2007, ApJ, 671, 748
Kalirai, J. S., Hansen, B. M. S., Kelson, D. D., Reitzel, D. B., Rich, R. M., & Richer, H. B. 2008, ApJ, 676, 594
Kalirai, J. S., Marigo, P., & Tremblay, P.-E. 2014, ApJ, 782, 17
Kalirai, J. S., Saul Davis, D., Richer, H. B., Bergeron, P., Catelan, M., Hansen, B. M. S., & Rich, R. M. 2009, ApJ, 705, 408
Kamath, D., Karakas, A. I., & Wood, P. R. 2012, ApJ, 746, 20
Karakas, A. I., Campbell, S. W., & Stancliffe, R. J. 2010, ApJ, 713, 374
Karakas, A. I., Fenner, Y., Sills, A., Campbell, S. W., & Lattanzio, J. C. 2006, ApJ, 652, 1240
Karakas, A. I. & Lattanzio, J. C. 2014, PASA, in press
Karakas, A. I., Lattanzio, J. C., & Pols, O. R. 2002, PASA, 19, 515
Karakas, A. I., Marino, A. F., & Nataf, D. M. 2014, ApJ, 784, 32
Lagarde, N., Charbonnel, C., Decressin, T., & Hagelberg, J. 2011, AA, 536, A28
Lattanzio, J. C. 1986, ApJ, 311, 708
Lau, H. H. B., Gil-Pons, P., Doherty, C., & Lattanzio, J. 2012, A&A, 542, A1
Lebzelter, T., Lederer, M. T., Cristallo, S., Hinkle, K. H., Straniero, O., & Aringer, B. 2008, A&A, 486, 511
Lederer, M. T., Lebzelter, T., Cristallo, S., Straniero, O., Hinkle, K. H., & Aringer, B. 2009, A&A, 502, 913
Lodders, K. 2003, ApJ, 591, 1220
Lodders, K., Palme, H., & Gail, H.-P. 2009, Landolt Börnstein, 4, 44
Marigo, P. 2001, A&A, 370, 194
—. 2002, A&A, 387, 507
Marigo, P. & Aringer, B. 2009, A&A, 508, 1539
Marigo, P., Bressan, A., Nanni, A., Girardi, L., & Pumo, M. L. 2013, MNRAS, 434, 488
Miglio, A., Brogaard, K., Stello, D., Chaplin, W. J., D'Antona, F., Montalbán, J., Basu, S., Bressan, A., Grundahl, F., Pinsonneault, M., Serenelli, A. M., Elsworth, Y., Hekker, S., Kallinger, T., Mosser, B., Ventura, P., Bonanno, A., Noels, A., Silva Aguirre, V., Szabo, R., Li, J., McCauliff, S., Middour, C. K., & Kjeldsen, H. 2012, MNRAS, 419, 2077
Mowlavi, N. 1999, A&A, 344, 617
Nataf, D. M. & Gould, A. P. 2012, ApJ, 751, L39
Nataf, D. M., Udalski, A., Gould, A., & Pinsonneault, M. H. 2011, ApJ, 730, 118
Ness, M., Freeman, K., Athanassoula, E., Wylie-de-Boer, E., Bland-Hawthorn, J., Asplund, M., Lewis, G. F., Yong, D., Lane, R. R., & Kiss, L. L. 2013, MNRAS, 430, 836
Nordhaus, J., Busso, M., Wasserburg, G. J., Blackman, E. G., & Palmerini, S. 2008, ApJ, 684, L29
Norris, J. E. 2004, ApJ, 612, L25
Nucci, M. C. & Busso, M. 2014, ApJ, 787, 141
Ortolani, S., Renzini, A., Gilmozzi, R., Marconi, G., Barbuy, B., Bica, E., & Rich, R. M. 1995, Nature, 377, 701
Palacios, A., Charbonnel, C., Talon, S., & Siess, L. 2006, A&A, 453, 261
Piersanti, L., Cristallo, S., & Straniero, O. 2013, ApJ, 774, 98
Pignatari, M., Herwig, F., Hirschi, R., Bennett, M., Rockefeller, G., Fryer, C., Timmes, F. X., Heger, A., Jones, S., Battino, U., Ritter, C., Dotter, A., Trappitsch, R., Diehl, S., Frischknecht, U., Hungerford, A., Magkotsios, G., Travaglio, C., & Young, P. 2013, ApJS, submitted
Piotto, G., Villanova, S., Bedin, L. R., Gratton, R., Cassisi, S., Momany, Y., Recio-Blanco, A., Lucatello, S., Anderson, J., King, I. R., Pietrinferni, A., & Carraro, G. 2005, ApJ, 621, 777
Porter, R. L., Ferland, G. J., Storey, P. J., & Detisch, M. J.

2012, MNRAS, 425, L28
Portinari, L., Casagrande, L., & Flynn, C. 2010, MNRAS, 406, 1570
Recio-Blanco, A., de Laverny, P., Kordopatis, G., Helmi, A., Hill, V., Gilmore, G., Wyse, R., Adibekyan, V., Randich, S., Asplund, M., Feltzing, S., Jeffries, R., Micela, G., Vallenari, A., Alfaro, E., Allende Prieto, C., Bensby, T., Bragaglia, A., Flaccomio, E., Koposov, S. E., Korn, A., Lanzafame, A., Pancino, E., Smiljanic, R., Jackson, R., Lewis, J., Magrini, L., Morbidelli, L., Prisinzano, L., Sacco, G., Worley, C. C., Hourihane, A., Bergemann, M., Costado, M. T., Heiter, U., Joffre, P., Lardo, C., Lind, K., & Maiorca, E. 2014, A&A, 567, A5
Reddy, B. E., Lambert, D. L., & Allende Prieto, C. 2006, MNRAS, 367, 1329
Rosenfield, P., Johnson, L. C., Girardi, L., Dalcanton, J. J., Bressan, A., Lang, D., Williams, B. F., Guhathakurta, P., Howley, K. M., Lauer, T. R., Bell, E. F., Bianchi, L., Caldwell, N., Dolphin, A., Dorman, C. E., Gilbert, K. M., Kalirai, J., Larsen, S. S., Olsen, K. A. G., Rix, H.-W., Seth, A. C., Skillman, E. D., & Weisz, D. R. 2012, ApJ, 755, 131
Saglia, R. P., Fabricius, M., Bender, R., Montalto, M., Lee, C.-H., Riffeser, A., Seitz, S., Morganti, L., Gerhard, O., & Hopp, U. 2010, A&A, 509, A61
Siess, L. 2010, A&A, 512, A10
Smith, C. L., Zijlstra, A. A., & Dinerstein, H. L. 2014, MNRAS, 441, 3161
Stancliffe, R. J. 2010, MNRAS, 403, 505
Stancliffe, R. J., Church, R. P., Angelou, G. C., & Lattanzio, J. C. 2009, MNRAS, 396, 2313
Stancliffe, R. J. & Jeffery, C. S. 2007, MNRAS, 375, 1280
Stanghellini, L. & Haywood, M. 2010, ApJ, 714, 1096
Stasińska, G., Richer, M. G., & McCall, M. L. 1998, A&A, 336, 667
Straniero, O., Domínguez, I., Cristallo, R., & Gallino, R. 2003, PASA, 20, 389
Straniero, O., Gallino, R., & Cristallo, S. 2006, Nuclear Physics A, 777, 311
Uttenthaler, S., Hron, J., Lebzelter, T., Busso, M., Palmerini, S., Schultheis, M., Käufl, H. U., Lederer, M. T., & Aringer, B. 2008, A&A, 478, 527
Uttenthaler, S., Hron, J., Lebzelter, T., Busso, M., Schultheis, M., & Käufl, H. U. 2007, A&A, 463, 251
Valenti, E., Zoccali, M., Renzini, A., Brown, T. M., Gonzalez, O. A., Minniti, D., Debattista, V. P., & Mayer, L. 2013, A&A, 559, A98
van Loon, J. T., Cioni, M.-R. L., Zijlstra, A. A., & Loup, C. 2005, A&A, 438, 273
van Loon, J. T., Gilmore, G. F., Omont, A., Blommaert, J. A. D. L., Glass, I. S., Messineo, M., Schuller, F., Schultheis, M., Yamamura, I., & Zhao, H. S. 2003, MNRAS, 338, 857
van Loon, J. T., Zijlstra, A. A., & Groenewegen, M. A. T. 1999, A&A, 346, 805
Vassiliadis, E. & Wood, P. R. 1993, ApJ, 413, 641
Ventura, P. & D'Antona, F. 2005a, A&A, 431, 279
—. 2005b, A&A, 439, 1075
Ventura, P., D'Antona, F., & Mazzitelli, I. 2000, A&A, 363, 605
Ventura, P., Di Criscienzo, M., Carini, R., & D'Antona, F. 2013, MNRAS, 431, 3642
Wallerstein, G. & Knapp, G. R. 1998, ARA&A, 36, 369
Weidemann, V. 2000, A&A, 363, 647
Whitelock, P. A., Feast, M. W., Marang, F., & Groenewegen, M. A. T. 2006, MNRAS, 369, 751
Zoccali, M., Hill, V., Lecureur, A., Barbuy, B., Renzini, A., Minniti, D., Gómez, A., & Ortolani, S. 2008, A&A, 486, 177
Zoccali, M., Renzini, A., Ortolani, S., Greggio, L., Saviane, I., Cassisi, S., Rejkuba, M., Barbuy, B., Rich, R. M., & Bica, E. 2003, A&A, 399, 931

This paper has been typeset from a TEX/ LATEX file prepared by the author.